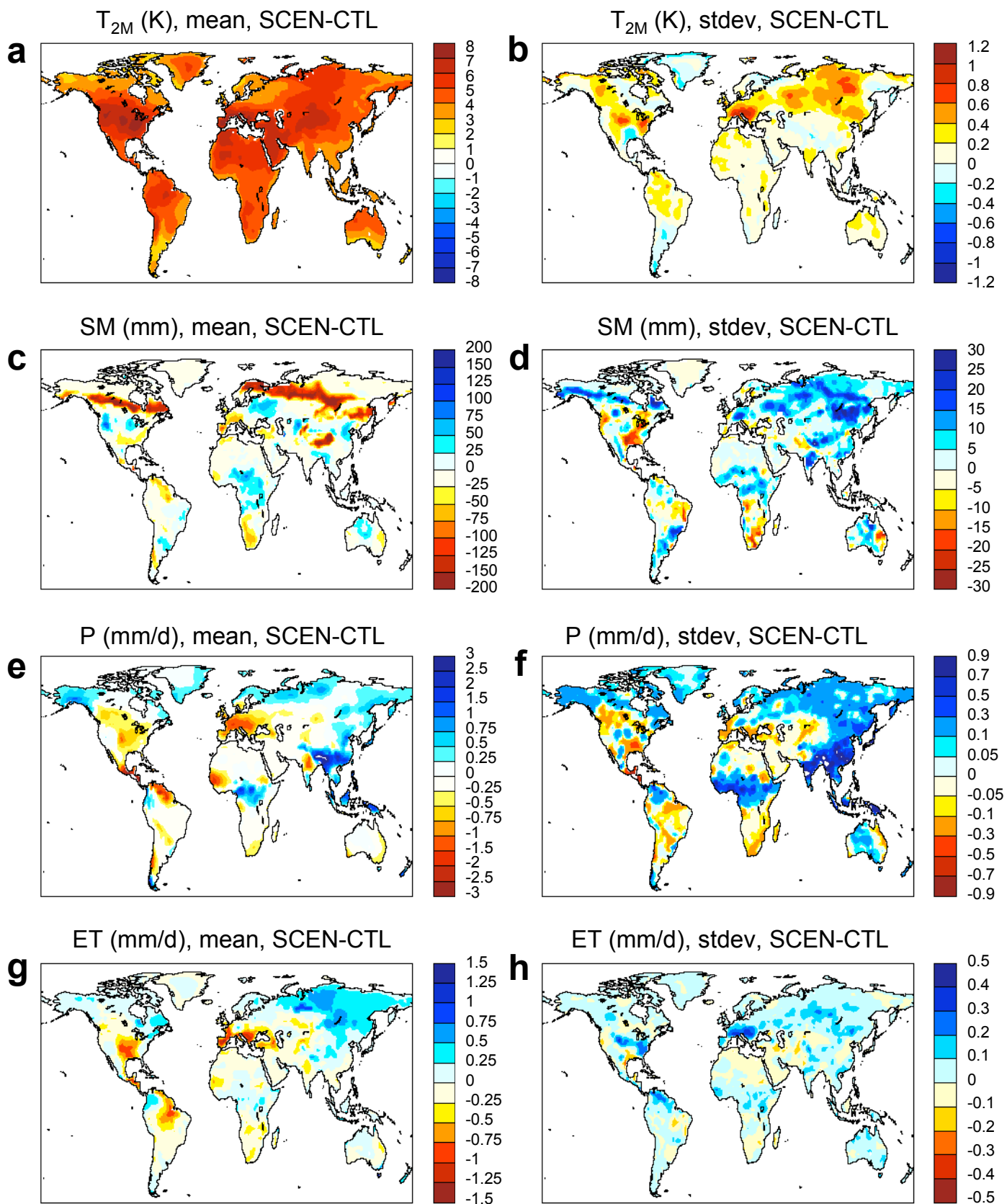
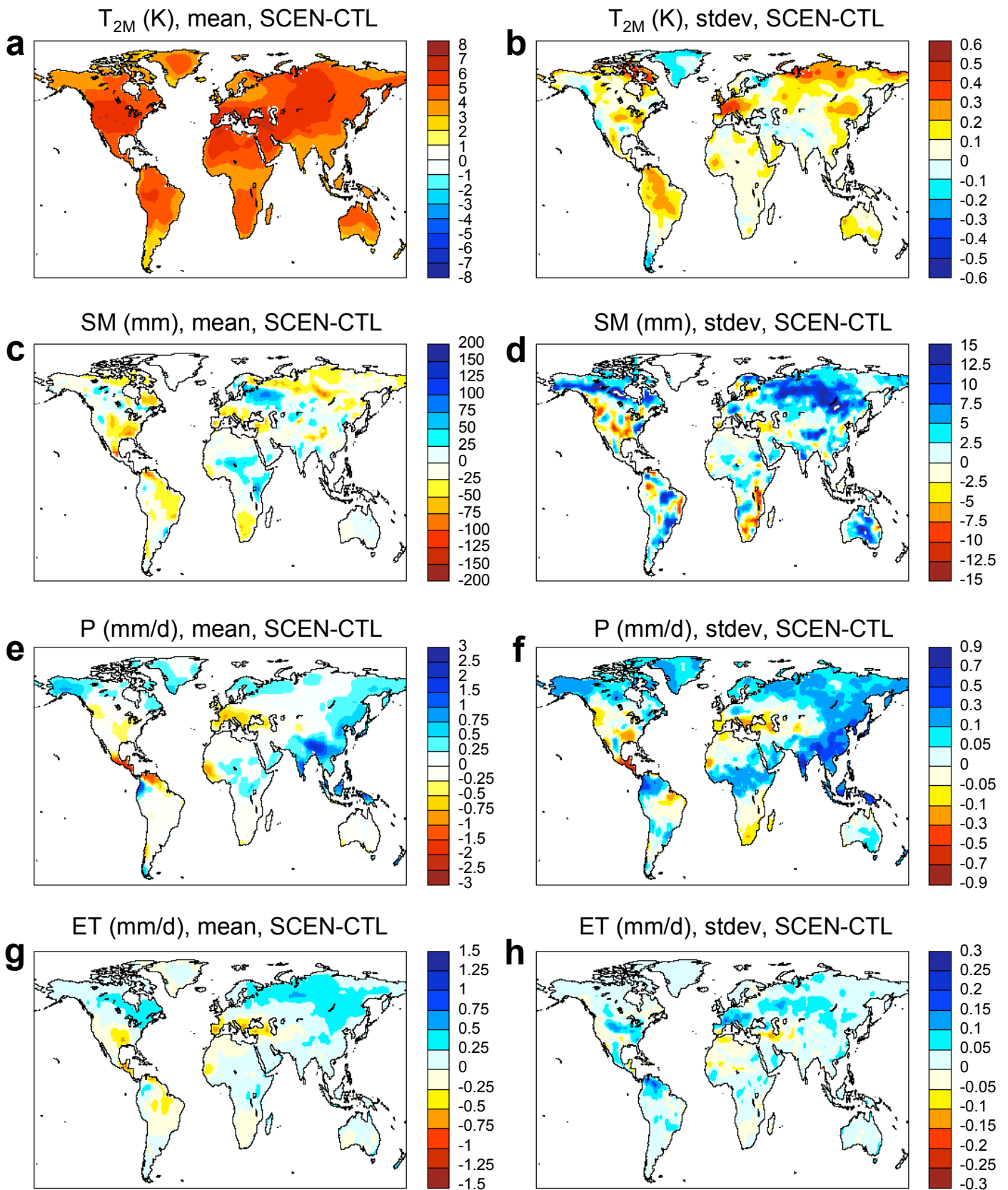


**Supplementary Figure 1:** Changes in mean (left) and interannual variability (standard deviation, right) of JJA temperature (a,b), soil moisture (c,d), precipitation (e,f), and evapotranspiration (g,h) between the CTL and SCEN experiments (SCEN-CTL). The underlying scenario is the SRES A2 and the periods correspond to CTL (1970-1989) and SCEN (2080-2099).



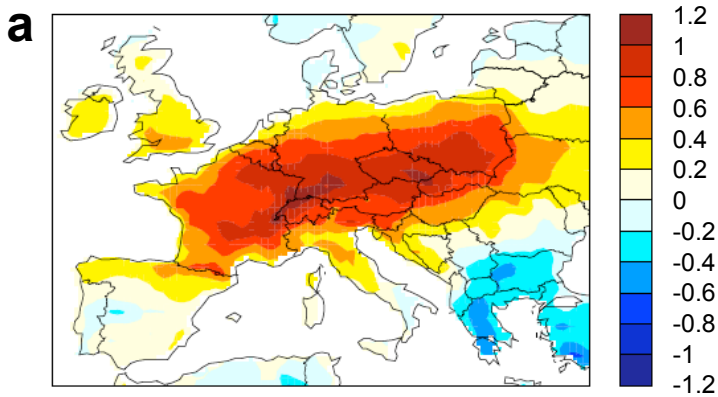
**Supplementary Figure 2:** As SF1, but for the mean of the following GCMs: ECHAM5, HADGEM1, and GFDL (see Supplementary Discussion 1).



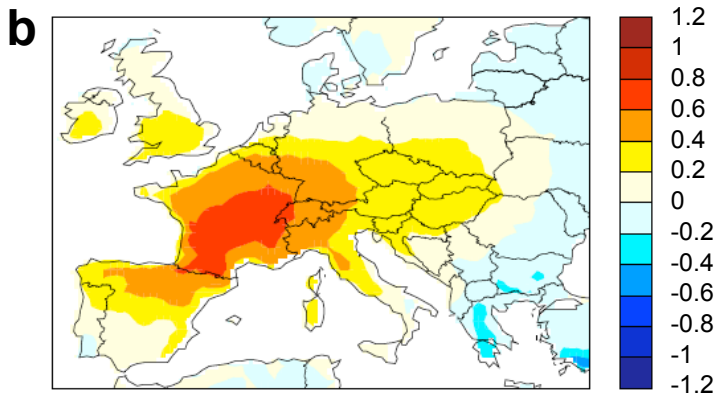
**Supplementary Figure 3:** As SF1 and SF2, but for the mean of all 12 considered GCMs (see Supplementary Discussion 1).

$T_{2M}$  (K), stdev

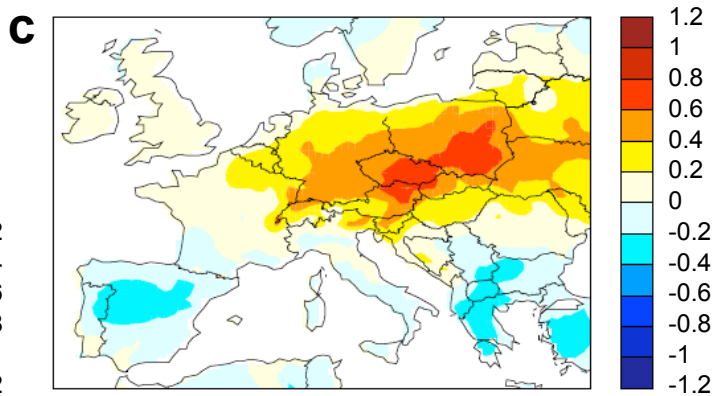
SCEN-CTL



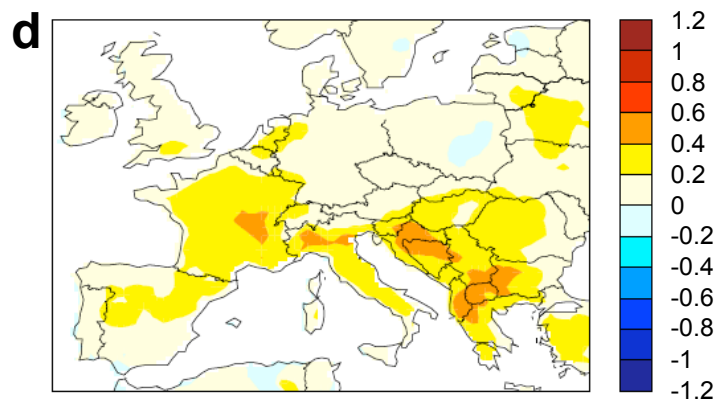
$SCEN_{UNCOUPLED} - CTL_{UNCOUPLED}$



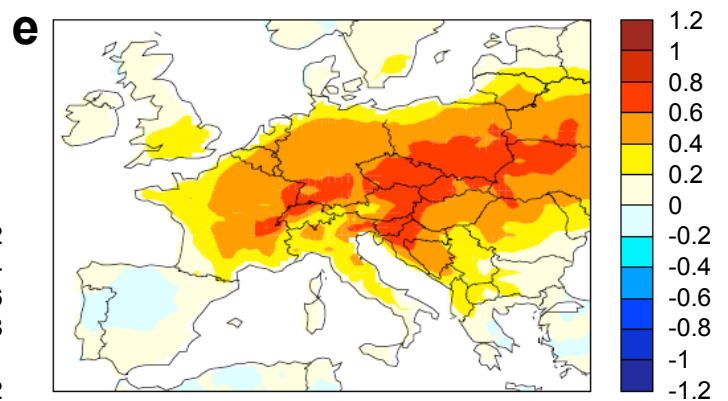
$(SCEN - SCEN_{UNC}) - (CTL - CTL_{UNC})$



$CTL - CTL_{UNCOUPLED}$



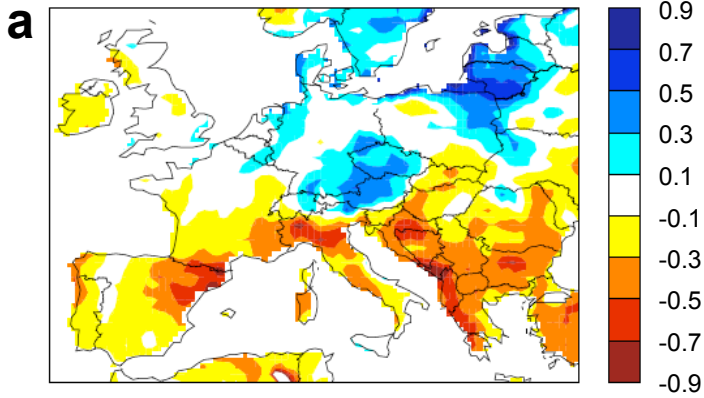
$SCEN - SCEN_{UNCOUPLED}$



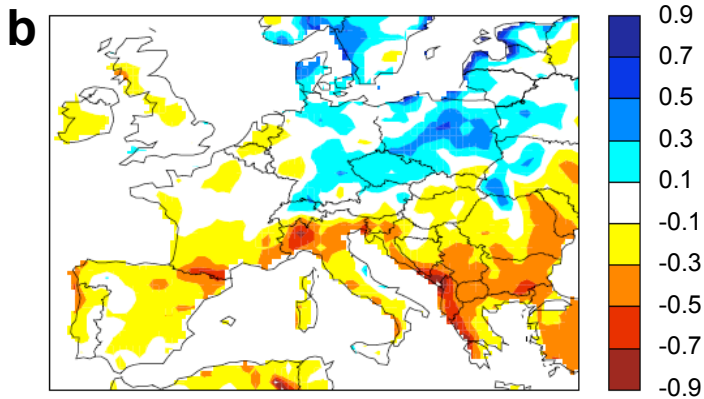
**Supplementary Figure 4:** Analysis of factors contributing to change in JJA temperature variability [K] between the CTL and SCEN simulations: (a) SCEN-CTL; (b)  $SCEN_{UNCOUPLED} - CTL_{UNCOUPLED}$ ; (c)  $(SCEN - SCEN_{UNCOUPLED}) - (CTL - CTL_{UNCOUPLED})$ ; (d)  $CTL - CTL_{UNCOUPLED}$ ; (e)  $SCEN - SCEN_{UNCOUPLED}$ . (See Supplementary Discussion 2).

# Precipitation (mm/d), stdev

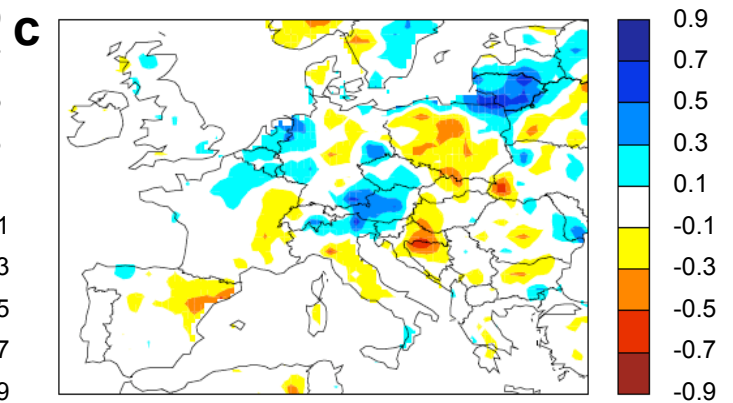
SCEN-CTL



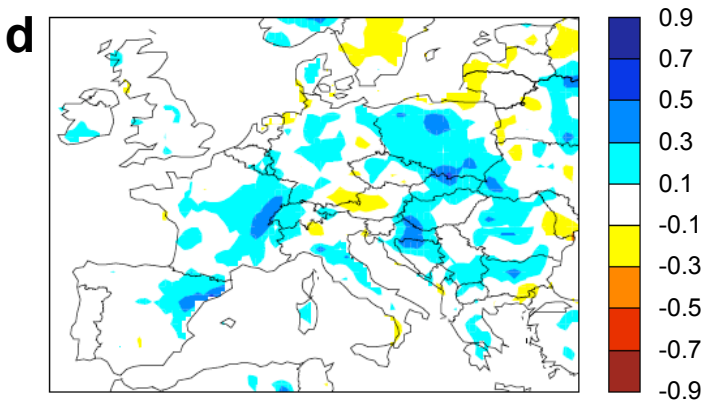
SCEN<sub>UNCOUPLED</sub>-CTL<sub>UNCOUPLED</sub>



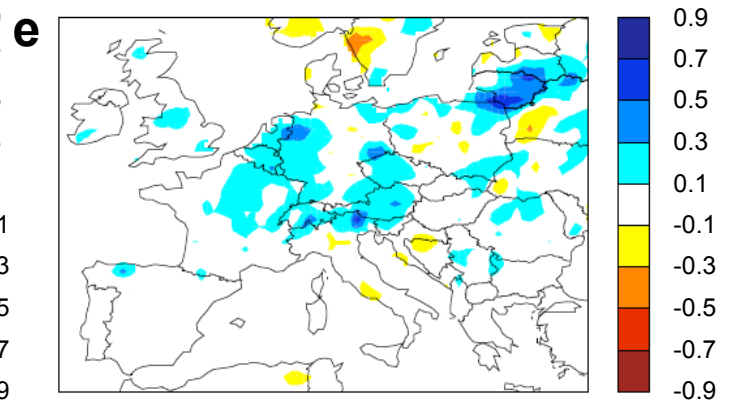
(SCEN-SCEN<sub>UNC</sub>)-(CTL-CTL<sub>UNC</sub>)



CTL-CTL<sub>UNCOUPLED</sub>



SCEN-SCEN<sub>UNCOUPLED</sub>



Supplementary Figure 5: As SF4, but for precipitation [mm/d].

**Supplementary Table 1: Set-up of simulations**

<b>Simulations</b>	<b>Driving GCM simulation</b>	<b>Simulation period</b>	<b>Analysis period*</b>	<b>Soil moisture state</b>
<b>CTL</b>	<b>HadAM3_CTL</b>	<b>1960-1989</b>	<b>1970-1989</b>	<b>Interactive</b>
<b>SCEN</b>	<b>HadAM3_A2</b>	<b>2070-2099</b>	<b>2080-2099</b>	<b>Interactive</b>
<b>CTL<sub>UNCOUPLED</sub></b>	<b>HadAM3_CTL</b>	<b>1960-1989</b>	<b>1970-1989</b>	<b>CTL climatology</b>
<b>SCEN<sub>UNCOUPLED</sub></b>	<b>HadAM3_A2</b>	<b>2070-2099</b>	<b>2080-2099</b>	<b>SCEN climatology</b>

\* Whenever mentioned, the “CTL time period” and “SCEN time period” refer to the analysis period.

### **Supplementary Discussion 1:**

#### **Consistency of mean climate and interannual variability of CTL and SCEN simulations with multi-model RCM and GCM experiments**

Within the framework of the European project PRUDENCE, the unperturbed simulations CTL and SCEN were compared with a number of state-of-the-art RCMs with regard to changes in summer climate variability (Vidale et al. 2006, hereafter referred to as V06). It was found that the identified increase of summer temperature variability in Central Europe is a very consistent feature in all RCMs, though the magnitude, exact spatial distribution and timing of the effect can somewhat differ. Moreover, V06 also showed that the decrease in mean soil moisture content and increase in soil moisture variability found in Central Europe was present in six RCMs analyzed in deeper detail (V06, Fig. 10). The increase in precipitation variability is present in most RCM simulations but less consistent than the increase in temperature variability (V06, Fig. 7).

In the Supplementary Figures 1-3 (hereafter referred to as SF1-3), we extend this analysis to IPCC AR4 GCM simulations. SF1-3 display changes in mean and standard deviation (see Methods) of the JJA temperature, soil moisture, precipitation, and evapotranspiration in the CTL and SCEN simulations (SF1), in the ECHAM5, HADGEM1, and GFDL GCMs (SF2), and in all 12 analyzed GCMs (SF3). For details concerning the GCM simulations, please refer to the Methods section. The choice of 3 GCMs displayed in SF2 corresponds to models characterized by high-quality circulation patterns in the northern mid- and high latitudes and in Europe (van Ulden and van Oldenborgh, 2006).

The comparison of SF1-3 shows that the analyzed GCMs present similar changes in mean climate and climate variability as the unperturbed RCM experiments (CTL, SCEN). They thus appear overall consistent with the results obtained in our modelling framework. Note that our experiments display a particularly close agreement with the three high-quality circulation GCMs concerning the exact magnitude of the changes in interannual summer variability (which are more damped in the 12-GCMs mean values).

#### *References:*

Vidale, P.L., Lüthi, D., Wegmann, R. & Schär, C. European climate variability in a heterogeneous multi-model ensemble. *Clim. Change*, conditionally accepted (2006).

van Ulden, A.O. & van Oldenborgh, G.J. Large-scale atmospheric circulation biases and changes in global climate simulations and their importance for climate change in Central Europe. *Atmos. Chem. Phys.*, **6**, 863-881 (2006).

## Supplementary Discussion 2:

### Analysis of factors contributing to changes in summer variability of temperature and precipitation

We present here a more detailed analysis of the factors contributing to changes in summer temperature and precipitation variability between the CTL and SCEN simulations. The relative contribution of changes in land-atmosphere coupling can be exactly defined using the following equation:

$$\begin{aligned} \text{SCEN-CTL} = & (\text{SCEN}_{\text{UNCOUPLED}} - \text{CTL}_{\text{UNCOUPLED}}) \\ & + [(\text{SCEN} - \text{SCEN}_{\text{UNCOUPLED}}) - (\text{CTL} - \text{CTL}_{\text{UNCOUPLED}})] \end{aligned} \quad (1)$$

Following (1), we find two main contributions to the change in temperature/precipitation variability:

- $[(\text{SCEN} - \text{SCEN}_{\text{UNCOUPLED}}) - (\text{CTL} - \text{CTL}_{\text{UNCOUPLED}})]$ : Change in land-atmosphere coupling contribution to temperature/precipitation variability between the CTL and SCEN climate conditions
- $(\text{SCEN}_{\text{UNCOUPLED}} - \text{CTL}_{\text{UNCOUPLED}})$ : Change in other factors (e.g. - but not exclusively - circulation patterns, sea surface temperatures)

The relative contributions of these two terms to the changes in summer temperature variability are displayed in Figure 1g,h as well as in combination with the terms  $(\text{SCEN} - \text{SCEN}_{\text{UNCOUPLED}})$  and  $(\text{CTL} - \text{CTL}_{\text{UNCOUPLED}})$  in the Supplementary Figure 4 (hereafter referred to as SF4). These figures show that the effect of the change in coupling is mainly located in Central and Eastern Europe, while effects of external factors appear stronger in France. Note that Fig. 1h (respectively, SF4c) is consistent with the analysis of changes in land-atmosphere coupling strength displayed in Fig. 2 and Fig. 3a,b.

The same analyses for changes in summer precipitation variability are displayed in Figure 4c,d and SF5. These figures show that the overall patterns of changes (decrease in the Mediterranean, increase in Central and Eastern Europe) appear related to external factors, while the particularly high increase of variability in the Alpine region is linked to changes in land-atmosphere coupling characteristics in the simulations.